DYNAMICS OF THE SMALL-SCALE TURBULENT MIXING IN CLOUDS: NUMERICAL EXPERIMENT.

Mirosław Andrejczuk, Szymon P. Malinowski
Warsaw University, Poland.

Wojciech W. Grabowski, and Piotr Smolarkiewicz
National Center for Atmospheric Research, USA.

1. INTRODUCTION

In recent years a growing attention is focused on small-scale properties of clouds (review in Valllancourt and Yau, 2000), especially on interaction of cloud particles with turbulence. In this research, however, turbulence is assumed as “given”, mostly by transport in spectral sense from large scales (according to the Kolmogorov theory). Little attention is being paid to production of turbulence in small scales by evaporative cooling of cloud liquid water in process of cloud-clear air mixing. There are, however, indications, that this production may affect smallest scales of turbulence resulting in e.g. anisotropy of cloudy filaments (Banat and Malinowski, 1999, later BM). In this paper we investigate such effects studying very small scales of turbulent mixing in clouds by detailed numerical modeling of dynamics, thermodynamics and microphysics with centimeter resolution. We assume that at these scales no subgrid TKE parameterization is necessary, thus dynamical setup of the model is similar to DNS simulations with decaying turbulence (Herring and Kerr, 1993).

We address the following questions:

1) When effects of LWC evaporation are important for TKE evolution in small scales and when can be neglected?
2) Does sedimentation of cloud droplets play an important role in smallest scales of turbulent mixing?
3) Is small-scale turbulence in clouds really isotropic?

The model used in these simulations is nonhydrostatic anelastic model by Smolarkiewicz and Margolin (1997) with moist thermodynamics by Grabowski and Smolarkiewicz (1996). Governing equations applied in the simulations can be written as follows:

$$\frac{D\mathbf{v}}{Dt} = -\nabla\pi + \mathbf{k}B + \mu\Delta\mathbf{v}\,;$$

$$\nabla\mathbf{v} = 0\,;$$

$$\frac{D\theta}{Dt} = \frac{L\theta_e}{c_p T_e} C_d + \mu_\theta \Delta\theta\,;$$

$$\frac{Dq_v}{Dt} = -C_d\,;$$

Corresponding author's address: Szymon P Malinowski, Institute of Geophysics, Warsaw University, ul. Pasteura 7, 02-093 Warszawa, Poland. e-mail: malina@fuw.edu.pl

respect to a hydrostatically balanced environment profile normalized by the density, $\mathbf{k}$-vertical unit vector, L, c_p - latent heat of condensation and specific heat at constant pressure, C_d - condensation rate; θ - potential temperature; q_v, q_c - water vapor and cloud water mixing ratios, μ μ_θ - viscosity and thermal diffusivity of the air. Index "e" denotes environmental undisturbed value and B is buoyancy defined as:

$$B = g\left(\frac{\theta-\theta_e}{\theta_0} - \varepsilon(q_v - q_{ve}) - q_c\right);$$

where $\varepsilon=R_v/R_d-1$, g- acceleration of gravity, θ_e-environmental temperature profile.

In the simulations we use two alternative parameterizations of microphysical processes:

1) Bulk parameterization, described by:

$$\frac{Dq_c}{Dt} = C_d\,;$$

2) Detailed parameterization, closely following Grabowski (1989), where we solve conservation equation for the number density function of cloud droplets $f(\mathrm{x},r,t)$ accounting for droplet sedimentation velocity. Here $f(x,r,t)dr$ is the concentration of droplets of radius between r and $r+dr$ at a given point $\mathbf{x}$ in space and at given time t evolving according the equation:

$$\frac{Df(\mathbf{x},r,t)}{Dt} = \frac{\partial\eta}{\partial t} - \frac{\partial}{\partial r}\left(f(\mathbf{x},r,t)\frac{dr}{dt}\right).$$

Here $D/Dt=\partial/\partial t + (\mathbf{v}-\mathbf{v}_t(r_i)\nabla$, $\mathbf{v}_t(r_i)$ is sedimentation velocity for the droplets of the radius r_i . dr/dt describes changes of the number density function due to diffusional growth of cloud droplets $dr/dt=AS/r$, $A=10^{-10}$ m^2/s, $S=q_v/q_{vs}$, is supersaturation, and $\partial\eta/\partial t$ is the nucleation rate. For the finite number of droplet size bins the condensation rate is given by:

$$C_d = \sum_i f_i \frac{dm_i}{dt}\,.$$

In the simulation presented here we use 16 classes of droplets (radius in range 0.78-24 μm). Sedimentation velocity is prescribed for each class according to Stokes law: $v_t(r)=Cr^2$, where C gives 1 cm/sec for 10 μm droplet.

2. SIMULATIONS

Initial dynamical setup was adopted from typical DNS simulations with decaying turbulence, formulated after Herring and Kerr (1993) in Fourier space:

$$\begin{pmatrix} u \\ v \\ w \end{pmatrix}(k,0) = Ak^2 \exp\left(-\left(\frac{k}{k_0}\right)^2\right)(\cos(2\pi\psi) + i\sin(2\pi\psi)).$$

Here u,v,w are velocity components, k – wavenumber, k_0=4.7568, A – depends on initial TKE, ψ- is random.

Nine numerical simulations have been performed. In all of them computational grid was 64*64*64 points with gridbox size 1cm. The choice of gridbox size was a compromise between DNS requirements (box size close to Kolmogorov scale) and parameterization of cloud water. Boundary conditions were cyclic in three dimensions. Potential temperature of the environmental air was set to 293K and relative humidity to 65%. Thermodynamical conditions should be representative to the top of the warm summer Cumulus cloud and resemble conditions in the cloud chamber (BM, Malinowski and Jaczewski 1999, later MJ).

Numerical simulations were grouped in three series:

1) Reference DNS with no LWC, dry mixing with passive scalar of concentration φ distributed initially according to the equation:

$$\chi(k,0) = k^2 \exp\left(-\left(\frac{k}{k_0}\right)^2\right)(\cos(2\pi\psi) + i\sin(2\pi\psi));$$

$$\phi = \begin{cases} 1 \; for \; F(\chi) \geq 0 \\ 0 \; for \; F(\chi) < 0 \end{cases};$$

where F denotes Fourier transform.

2) Mixing of cloud with clear air, bulk parameterization of LWC, initial cloud distribution (LWC>0 and saturated air) was the same as above, initial value of LWC was 3g/kg, to give zero initial buoyancy;

3) Mixing of cloud with clear air, detailed parameterization of LWC, initial distribution and value of LWC as in case 2, three classes of droplets present: diameters of 7μm (contains 25% of LWC), 8.5μm (contains 50% of LWC) and 10μm (contains 25% of LWC).

In each of the series three numerical experiments for three initial values of initial velocities (given by constant A) corresponding to initial mean TKE equal to $2.16 \cdot 10^{-2}$, $5.4 \cdot 10^{-3}$ and $2.16 \cdot 10^{-4}$ m^2s^2 respectively, were done. These values of TKE in small scales correspond to high, medium and low turbulence levels in clouds.

For high turbulence runs lasted about 20s of model time, for medium and low turbulence runs lasted 25s, after this time practically all phase change processes were completed.

3. RESULTS

Results of these experiments are summarized in figures 1-7 where time evolutions of various features of modeled flow are plotted.

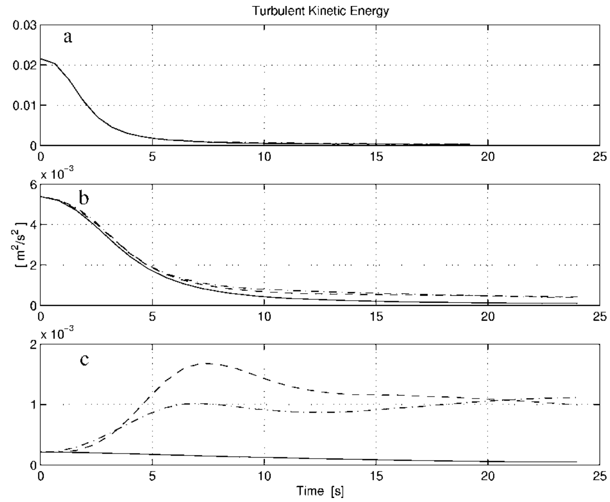

Figure 1. Temporal evolution of turbulent kinetic energy. (a) - high initial TKE, (b) - medium initial TKE. (c) - low initial TKE. Solid line - reference dry case, dash dot line - bulk microphysics, dashed line - detailed microphysics.

In Fig.1 evolution of TKE is analyzed. For the case of high initial TKE (Fig. 1a) evaporation of liquid water, practically does not influence energy of the flow. We see that in the first second, when initial whirls develop into smaller eddies; TKE dissipation (slope of TKE plot) increases, then reaches its maximum, and after 2.5s decreases with lessening level of TKE. After 10s, where most of initial TKE dissipated, some difference between dry and wet cases can be seen. For medium initial TKE (Fig. 1b), kinetic energy produced by evaporation of LWC significantly influences motion after 5s. After 12s flows with mixing/evaporation are substantially more vigorous than the dry reference. There is not much difference between bulk and detailed microphysics.

For low initial TKE (Fig. 1c) we see dramatic differences between all three investigated cases. While in reference dry flow systematic dissipation of TKE governs the flow, production of TKE due to phase change and buoyancy forces dominate both wet cases. Note, that temporal evolution of TKE differs significantly between bulk and detailed runs. Between 4th and 15th second of the experiment flow with detailed microphysics is more vigorous than with bulk microphysics. This shows, that droplet sedimentation may significantly influence small-scale mixing, supporting experimental results by BM and MJ. This is, however, only qualitative statement that may be fully confirmed by detailed simulations resolving evolutions of individual droplets.

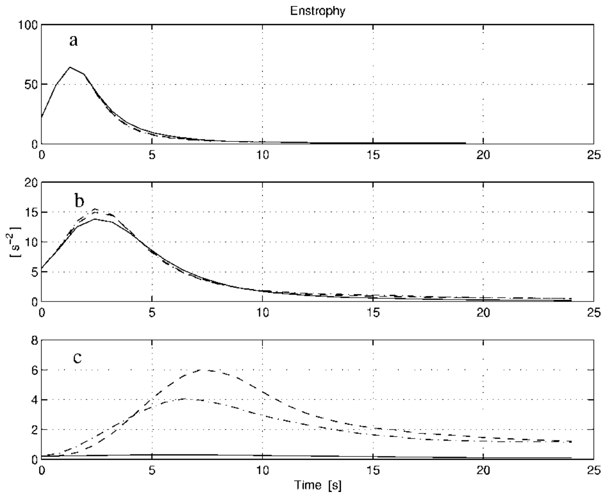

Figure 2. Temporal evolution of mean enstrophy (details as in Fig.1).

In Fig.2 evolution of mean enstrophy, ($E_n=0.5<\omega^2>$, where ω is vorticity) is presented. Enstrophy can be interpreted as index of intensity of turbulent vortices We see here small differences between wet and dry cases for low and medium initial TKE (Figs 2a and 2b, and huge differences for low TKE (Fig. 2c). Note, that for evaporative cooling in low and moderate initial TKE enstrophy has after 10s comparable levels, suggesting existence of comparable turbulent vortices. As for TKE, in low turbulence droplet sedimentation influences enstrophy evolution (Fig.2c).

Fig.3 presents temporal evolution of the Taylor microscale Reynolds number R_λ, which combines both TKE and enstrophy in one parameter describing microstructure of the flow:

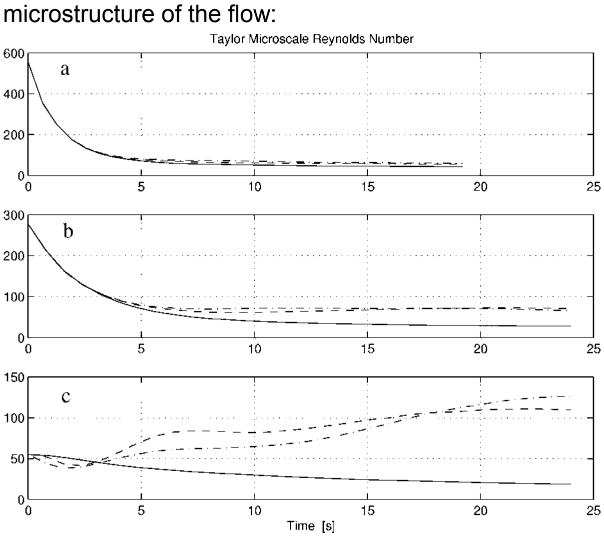

Figure 3. Time evolution of Taylor microscale Reynolds number (details as in Fig.1).

$$R_\lambda = \frac{TKE}{\mu} * \left(\frac{10}{3E_n}\right)^{1/2}$$

We see here, that after 20s R_λ for "wet" cases is comparable for all three initial values of TKE suggesting that this turbulence microstructure is governed more by the LWC evaporation than the initial value of TKE. Note that buoyancy produced by evaporation acts in vertical, which suggests that anisotropy of some turbulent properties should be observed.

In Figs. 4 and 5 evolutions of Taylor microscales defined by equation:

$$\lambda_i^2 = \left\langle u_i^2 \right\rangle / \left\langle \left(\frac{\partial u_i}{\partial x_i}\right)^2 \right\rangle$$

are plotted for velocity components u and w.

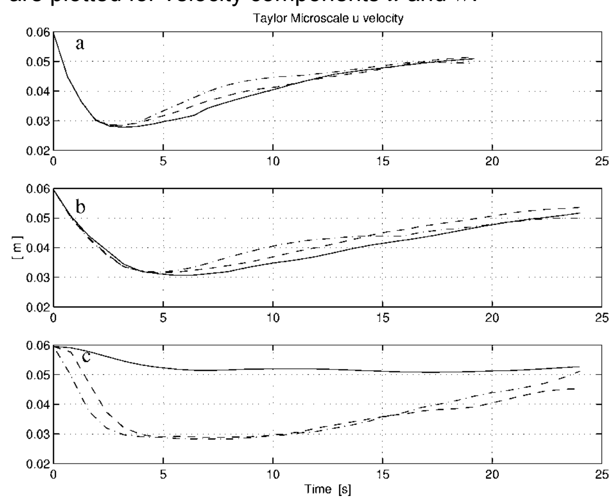

Figure 4. Time evolution of Taylor microscale for u (see caption of Fig.1 for details).

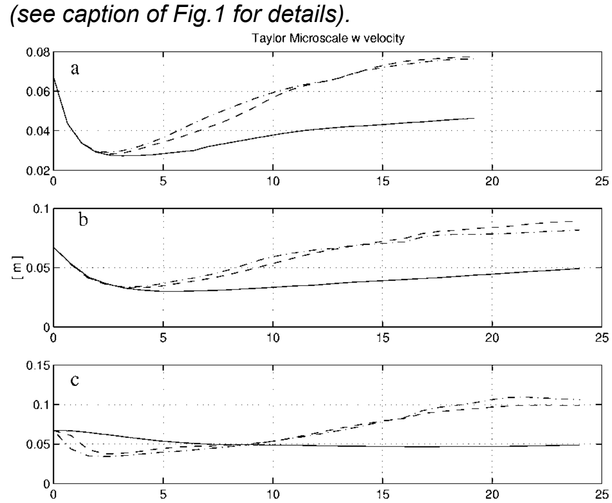

Figure 5. Temporal evolution of Taylor microscale for w (see caption of Fig.1 for details).

We see here (Fig. 4), that after 20s the horizontal Taylor microscale is comparable for all 9 flows and riches value of order of 5cm. Vertical Taylor microscale (Fig.5) at this time for the reference dry case reaches also 5 cm, while for both wet cases it becomes up to two times larger (from 8 to 10cm in Figs. 5a, b and c). Note, that this result is in agreement with findings of MB who show that filaments created by turbulent mixing of cloud and clear air are elongated in vertical.

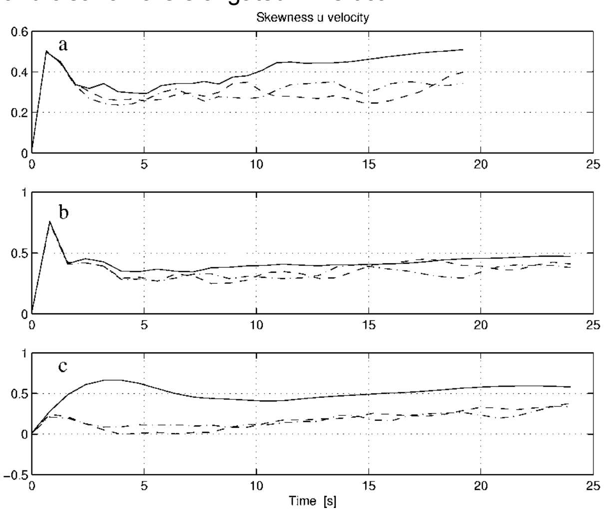

Figure 6. Temporal evolution of velocity-derivative skewness for u (details as in Fig.1).

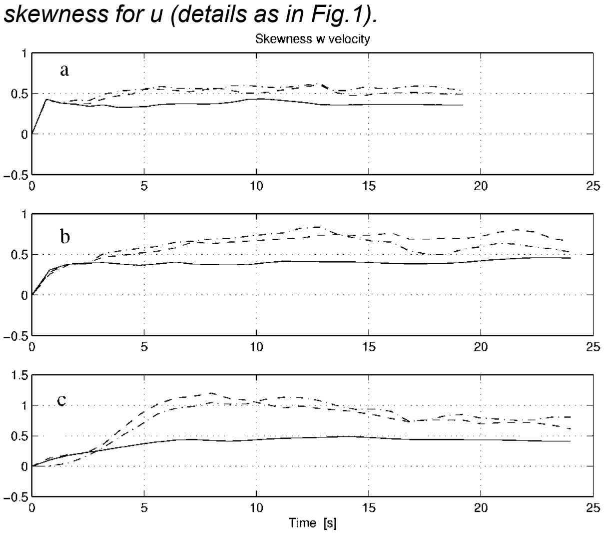

Figure 7. Temporal evolution of velocity-derivative skewness for w (details as in Fig.1).

Difference between properties of turbulence in horizontal and vertical directions are clear also in Figs. 6 and 7, presenting velocity derivative skewness:

$$S_i = \left\langle \left(\frac{\partial u_i}{\partial x_i} \right)^3 \right\rangle / \left\langle \left(\frac{\partial u_i}{\partial x_i} \right)^2 \right\rangle^{-3/2}$$

of horizontal (Fig.6) and vertical (Fig.7) component of turbulent velocity.

4. CONCLUSIONS.

Answering questions asked in the introduction we might conclude that:

1) At high initial values of TKE small-scale mixing with evaporative cooling does not significantly affect TKE evolution, while for moderate and small values of initial TKE this influence is substantial or even dominating. It is interesting that Taylor microscale Reynolds number after 20 s reaches largest values for wet cases with small initial.
2) Sedimentation of droplets may be important for low levels of initial TKE.
3) Buoyancy production in cloud-clear air mixing causes that even smallest scales of turbulence are highly anisotropic.

5. ACKNOWLEDGMENTS:

This research was supported by grant No. 6 P04D 027 19 of the Polish Committee for Scientific Research. Computations were performed at the Interdisciplinary Center for Mathematical and Computational Modeling of Warsaw University.

6. REFERENCES:

Banat, P and S.P. Malinowski, 1999: Properties of the turbulent cloud-clear air interface observed in the laboratory experiment. *Phys. Chem. Earth (B),* **24**, 741-745.

Grabowski, W. W., 1989: Numerical experiments on the dynamics of the cloud-environment interface: Small cumulus in a shear free environment. *J. Atmos. Sci*., **49**, 3513-5341.

Grabowski, W.W., and P.K. Smolarkiewicz, 1996: Two-time-level semi-Lagrangian modeling of precipitating clouds. *Mon. Wea. Rev.*, **124**, 487-497.

Herring J.R. and R.M. Kerr, 1993: Development of enstrophy and spectra in numerical turbulence. *Phys. Fluids A* **5** (11), 2792-2798.

Malinowski, S.P. and A. Jaczewski, 1999: Laboratory investigation of droplet concentration at the cloud-clear interface. *Phys. Chem. Earth (B),* **24**, 477-480.

Smolarkiewicz, P.K., and L.G. Margolin, 1997: On forward -in-time differencing for fluids: An Eulerian / semi-Lagrangian nonhydrostatic model for stratified flows. *Atmos.-Ocean*, **35,** 127-152

Vaillancourt, P.A. and M. K. Yau, 2000: Review of particle-turbulence interactions and consequences for cloud physics. *Bull. Amer Meteorol. Soc.*, **81** (2): 285-298.